ORIGINAL ARTICLE

Cell Proliferation WILEY

Direct inhibitory effect on viral entry of influenza A and SARS-CoV-2 viruses by azithromycin

Xiaohong Du[1,2,3] | Xiangyang Zuo[1,2] | Fang Meng[1,2] | Chenfeng Han[1,2] |
Wei Ouyang[4] | Yu Han[4] | Yayun Gu[1,2] | Xin Zhao[1,2] | Feng Xu[4] (iD) |
Frank Xiaofeng Qin[1,2] (iD)

[1]Center of Systems Medicine, Institute of Basic Medical Sciences, Chinese Academy of Medical Sciences and Peking Union Medical College, Beijing, China

[2]Suzhou Institute of Systems Medicine, Suzhou, China

[3]Institute of Clinical Medicine Research, the Affiliated Suzhou Hospital of Nanjing Medical University, Suzhou Science and Technology Town Hospital, Suzhou, China

[4]Department of Infectious Diseases, Second Affiliated Hospital of Zhejiang University School of Medicine, Hangzhou, China

Correspondence

Frank Xiaofeng Qin, Center of Systems Medicine, Institute of Basic Medical Sciences, Chinese Academy of Medical Sciences and Peking Union Medical College, Beijing 100005, China.
Email: fqin1@foxmail.com

Feng Xu, Department of Infectious Diseases, The Second Affiliated Hospital, Zhejiang University School of Medicine, No. 88 Jiefang Road, Hangzhou, 310009, China.
Email: xufeng99@zju.edu.cn

Funding information

This work was supported by: The Key Program for Innovative Drug Development of China (Grant 2015ZX09102023); Jiangsu Provincial Natural Science Foundation (Grant BK20171232); The National Natural Science Foundation of China (Grant 81701567, 81773058, 31800726 and 81970004); The Chinese Academy of Medical Sciences Initiative for Innovative Medicine (Grant CAMS-I2M, 2016-I2M-1-005); National grand Foreign Experts projects (culture and education) (Grant GDW20181100054); National grand Foreign Experts projects (G20190001633 and G20190001639).

Abstract

Objectives: Using strategy of drug repurposing, antiviral agents against influenza A virus (IAV) and newly emerging SARS-coronavirus 2 (SARS-CoV-2, also as 2019-nCoV) could be quickly screened out.

Materials and Methods: A previously reported engineered replication-competent PR8 strain carrying luciferase reporter gene (IAV-luc) and multiple pseudotyped IAV and SARS-CoV-2 virus was used. To specifically evaluate the pH change of vesicles containing IAV, we constructed an A549 cell line with endosomal and lysosomal expression of pHluorin2.

Results: Here, we identified azithromycin (AZ) as an effective inhibitor against multiple IAV and SARS-CoV-2 strains. We found that AZ treatment could potently inhibit IAV infection in vitro. Moreover, using pseudotyped virus model, AZ could markedly block the entry of SARS-CoV-2 in HEK293T-ACE2 and Caco2 cells. Mechanistic studies further revealed that such effect was independent of interferon signalling. AZ treatment neither impaired the binding and internalization of IAV virions, nor the viral replication, but rather inhibited the fusion between viral and vacuolar membranes. Using a NPC1-pHluorin2 reporter cell line, we confirmed that AZ treatment could alkalize the vesicles containing IAV virions, thereby preventing pH-dependent membrane fusion.

Conclusions: Overall, our findings demonstrate that AZ can exert broad-spectrum antiviral effects against IAV and SARS-CoV-2, and could be served as a potential clinical anti-SARS-CoV-2 drug in emergency as well as a promising lead compound for the development of next-generation anti-IAV drugs.

1 | INTRODUCTION

Influenza viruses, members of the *Orthomyxoviridae* family, are persistent and seasonal epidemical health threats to human beings.[1] Influenza viruses consist of influenza A, B, C and D virus (IAV, IBV, ICV, IDV).[2] IAV is the pathogen of most seasonal influenza and influenza pandemics.[1] Classification of IAV is based on the antigenic properties of hemagglutinin (HA) and neuraminidase (NA). The H1N1 and H3N2 subtypes cause seasonal and pandemic infections, while the highly pathogenic avian H5N1 and H7N9 subtypes cause severe mortality.[3]

Unlike IAV, coronaviruses rarely cause serious pandemics, but beta coronaviruses have caused three zoonotic outbreaks (SARS-CoV in 2002-2003,[4] MERS-CoV in 2012[5] and SARS-CoV-2 in the late 2019[6]) in the first decades of the 21st century. Especially, the newly emerged SARS-CoV-2, pathogen of coronavirus disease 2019 (COVID-19), has rapidly become a global pandemic with over 47 million confirmed COVID-19 cases and over 1.2 million confirmed deaths by 5 November 2020 (covid19.who.int). Unfortunately, there are still no regulatory-approved drugs for COVID-19 patients. Although remdesivir and chloroquine have shown potential antiviral ability against SARS-CoV-2 in vitro,[7] the clinical antiviral effects and safety have not been fully verified.[8,9] Interestingly, azithromycin (AZ) showed synergistic anti-SARS-CoV-2 effect with hydroxychloroquine in vitro, but the mechanism is still unclear.[8]

The two conventional strategies to fight against influenza pandemics and epidemics are small-molecule antiviral drugs and vaccines.[10-13] However, influenza vaccines must be reformulated yearly to match with the antigens of circulating viruses.[14,15] Moreover, vaccine production usually lags behind identification of circulating virus for 6 months.[15]

Drug repurposing, also known as drug rescue or drug repositioning, refers to the re-examination of existing drugs for new therapeutic purposes.[16] Compared to conventional drug development, drug repurposing possesses significant advantages, such as lower risk of failure and shorter research and development time period due to the known pharmacokinetic properties, tolerance and toxicity of approved drugs.

In the present study, we reported the repurposing of AZ, a macrolide antibiotic, is a potential antiviral drug candidate for high-pathogenic IAV and newly emerging SARS-CoV-2. Macrolide antibiotics have well-established antibacterial,[17,18] anti-inflammatory effects[19-21] and certain antiviral effects against rhinovirus.[22-24] In addition, it has been recently reported that AZ could reduce Zika viral proliferation and cytopathic effects induced by the virus in glial cell lines and human astrocytes.[25] Furthermore, Li et al also demonstrated that AZ upregulates the expression of IFN-I/III and some of their downstream interferon-stimulated genes (ISGs) in response to Zika virus infection.[26]

In spite of the reported antiviral activity of AZ, the mechanism of AZ against viral infection is still not understood. In the current study, we established an A549 cell line with endosome-specific pHluorin2 expression to quantitatively analyse the effect of AZ on acidification of vesicles containing virions and found that AZ could exert antiviral activity through disturbing the acidification of endosomes containing IAV. Moreover, we found that AZ could inhibit the entry of SARS-CoV-2 pseudovirus in HEK293T-ACE2 and Caco2 cells. Taken together, we evaluated the previously unknown antiviral mechanism of AZ against IAV and SARS-CoV-2, and provide a potential candidate for future clinical drug application against IAV and SARS-CoV-2.

2 | METHODS AND MATERIALS

2.1 | Cells, virus and reagents

Human cervix adenocarcinoma (Hela), adenocarcinomic human alveolar basal epithelial cells (A549), human embryonic kidney cells (HEK293T) and human colon adenocarcinoma cell (Caco2) were obtained from American Type Culture Collection and maintained in complete DMEM medium (containing 2 mmol/L L-Glutamine, 10% foetal bovine serum (Thermo Fisher Scientific), 100 μg/mL streptomycin and 100 U/mL penicillin) at 37°C with 5% CO_2 incubation. The interferon receptor knockout (IFNAR1 KO) HEK293T cells and retinoic acid-inducible gene-I (RIG-I) KO HEK 293T cells were kept in our laboratory. The influenza virus strains used in this study were A/WSN/33(H1N1) (WSN), which was kept in our laboratory. The IAV-luc (PR8) strain was a gift from Prof. Ling Chen (Guangzhou Institutes of Biomedicine and Health, Chinese Academy of Sciences). AZ and erythromycin were obtained from BBI Life Sciences. Ribavirin was obtained from Solarbio. Oseltamivir, midecamycin, spiramycin, acetylspiramycin, clarithromycin, dirithromycin, tamoxifen, fluvastatin, fluoxetine and clemastine were obtained from MedChemExpress. Amiodarone, amantadine, roxithromycin, delphinidin and bafilomycin A1 were obtained from Sigma. Chloroquine (CQ) and amlodipine (Norvasc) were obtained from Sangon Biotech.

2.2 | Screening with IAV-luc

Briefly, A549 cells were pre-treated for 8 hours with the indicated drugs, infected with IAV-luc at an MOI of 0.01 for 24 hours. Then, the viral titres were measured by detecting the luciferase activity of supernatant by a microplate reader.

2.3 | Establishment of HEK293T-ACE2 cells

As ACE2 has been identified as the host receptor of SARS-CoV and SARS-CoV-2, we constructed the human ACE2 stable expressed HEK293T (HEK293T-ACE2) with lentiviral mediated gene transduction.

2.4 | Cytotoxicity assay

The cytotoxicity of the candidate drugs in A549 and HEK293T-ACE2 cells was detected with the cell counting kit-8 (CCK8) after 72 hours treatment.

2.5 | Pseudovirus preparation

For IAV, VSV and Ebola entry assays, pseudovirus based on HIV were prepared as previously reported.[27] Briefly, HEK 293T cells were transfected with pNL4-3-luc R⁻E⁻ and IAV HA/NA, VSV-G or Ebola-GP expressing plasmid. The HA and NA expression vectors of A/chicken/Hubei/327/2004(H5N1) and A/Anhui/1/YK_RG25/2013(H7N9) were gifts from Yi Shi (Institute of Microbiology, Chinese Academy of Sciences). For SARS-CoV and SARS-CoV-2 entry assays, pseudovirus based on murine leukaemia virus (MLV) were prepared by transection of HEK293T with spike protein expressing plasmid, pCgp and pRV107G-luc. The SARS-CoV and SARS-CoV-2 spike protein expression vectors were constructed by PCR from the pcDNA3.1-SARS-S-P2A-eGFP and pcDNA3.1-SARS-CoV-2-S-P2A-eGFP (Molecular Cloud No. MC_0101088 and MC_0101087) with 19aa deletion in C-terminator. The mutant SARS-CoV-2 spike expression vectors were constructed by PCR from wild-type (WT) spike expression vector with mutagenesis kit (TOYOBO).

2.6 | Pseudovirus entry assay

For entry assays, pseudovirus entry assay was carried out as previously reported.[27] Briefly, A549, HEK293T-ACE2 or Caco2 cells were pre-treated for 8 hours with the indicated drugs, infected with pseudovirus for 72 hours and lysed for the luciferase assay.

2.7 | IAV minigenome assay

Viral polymerase activity was assessed using an experimentally optimized minigenome assay with viral polymerase expression vectors (pcDNA-NP, pcDNA-PB1, pcDNA-PB2 and pcDNA-PA, in a 1:1:1:1 ratio), a viral RNA firefly luciferase reporter construct (minigenome) and Renilla luciferase expression plasmid as an internal transfection control, as described previously.[28]

2.8 | Quantitative real-time PCR

Total RNA was obtained using the Ultrapure RNA kit (cwbiotech). cDNAs were transcribed using HiFiScript cDNA synthesis kit (cwbiotech). Real-time PCR was performed using the Fast SYBR Green PCR Master Mix. The relative expression of each gene was normalized to the expression of GAPDH or ribosomal protein L32. The primer sequences for human: IFNB1 sense-5′- CCTACAAAGAAGCAGCAA and antisense-5′- TCCTCAGGGATGTCAAAG; ISG54 sense-5′- GGAGGGAGAAAACTCCTTGGA and antisense-5′- GGCCAGTAGGTTGCACATTGT; CCL5 sense-5′- ATCCTCATTGCTACTGCCCTC and antisense-5′- GCCACTGGTGTAGAAATACTCC; GAPDH sense-5′- GAACGGGAAGCTCACTGG and antisense-5′- GCCTGCTTCACCACCTTCT; L32 sense-5′- TTAAGCGAAACTGGCGGAAAC and antisense-5′- TTGTTGCTCCCATAACCGATG. The primer sequences for WSN: NP sense-5′- GGATCAAGTGAGAGAGAGCCG and antisense-5′- ACGGCAGGTCCATACACACAG.

2.9 | IAV labelling

To locate or quantitative analyse the IAV particle, WSN stocks were diluted in PBS to 0.1 mg/mL and labelled with Dil (Thermo Fisher Scientific) or R18 (Thermo Fisher Scientific) and SP-DiOC18 (Thermo Fisher Scientific) at RT for 1 hour. The labelled virus particles were filtered through a 0.22 μm-pore filter (Millipore) and stored at 4°C in the dark till used.

2.10 | IAV binding, internalization and membrane fusion assay

For binding assay, A549 cells were pre-treated with indicated drugs at 37°C for 2 hours and incubated with Dil-labelled WSN at 4°C for 1 hour.

For internalization assay, A549 cells were transfected with EGFP-RAB5A or EGFP-RAB7A expression vector. A549 cells were pre-treated with indicated drugs 24 hours after transfection at 37°C for 2 hours and incubated with Dil-labelled WSN at 4°C for 1 hour, and then incubated at 37°C for 45 minutes.

For membrane fusion assay, a lipophilic dye-based fluorescence dequenching assay using R18 (red) and SP-DiOC18 (green, fixable) was used.[29] A549 cells were pre-treated with the indicated drugs at 37°C for 2 hours and incubated with R18/SP-Dioc18 labelled WSN in infection medium at 4°C for 1 hour, and incubated at 37°C for 1 hour. Then, the cells were washed with ice-cold PBS, fixed with 4% formaldehyde for 10 minutes, rewashed with PBS and stained with DAPI. The images were captured with a confocal microscope (Leica TCS SP8) and analysed with ImageJ (Image J_1.51j8).

2.11 | Endosome acidification assay

Total acidification was assessed with Lyso-Tracker Red (Beyotime) as a probe for low-pH organelles. Cells were pre-treated with the indicated drugs at 37°C for 2 hours and then incubated with 50 nmol/L Lyso-Tracker Red for 30 minutes. Cells were analysed by fluorescence microscopy.

The pH calibration curve was generated as described previously.[30,31] The buffers for generating the pH calibration curve
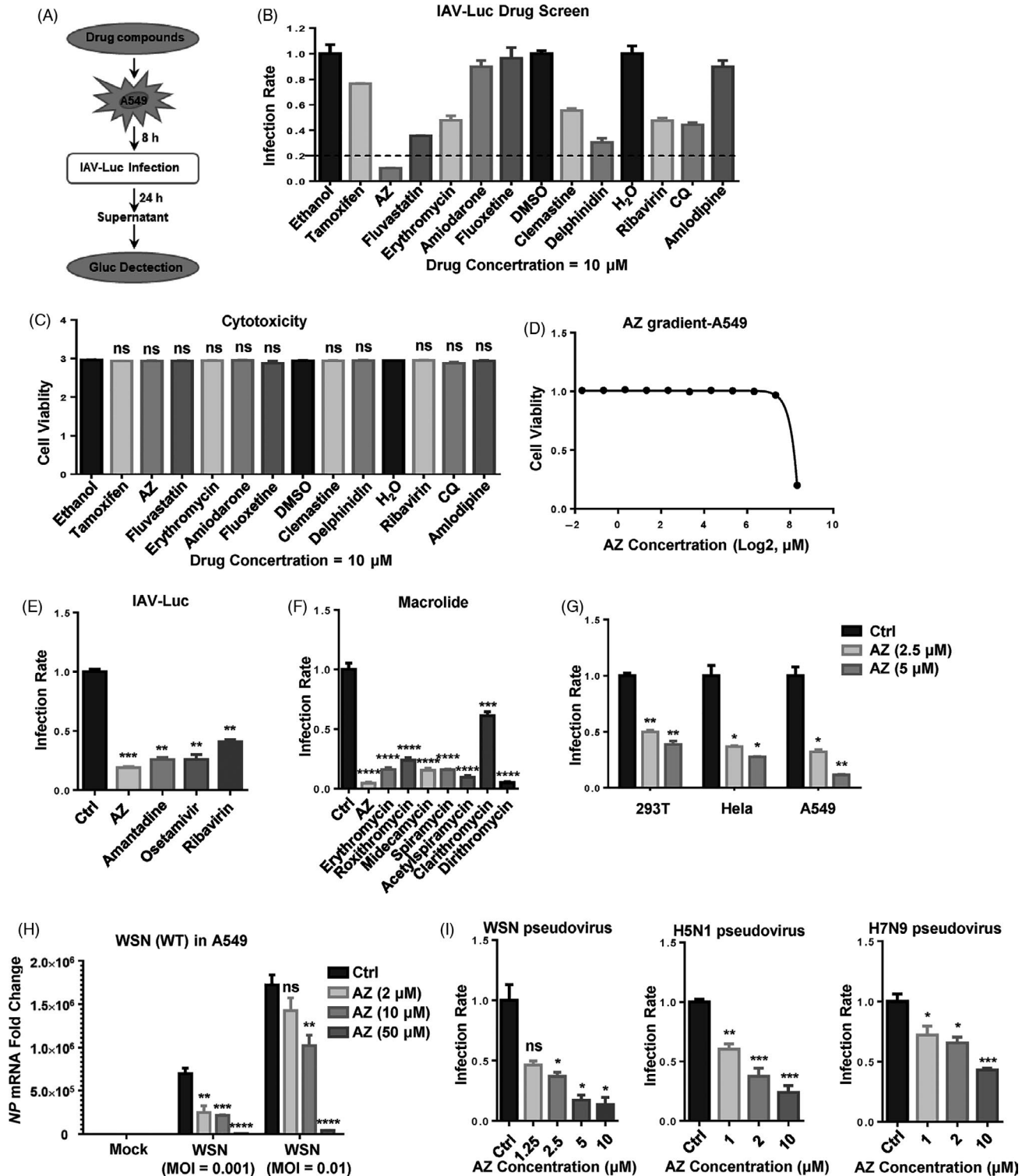
FIGURE 1 AZ is identified as a potential inhibitor of IAV in vitro. A, The flow chart of IAV-luc assay. B and C, The relative inhibitory rate of on IAV-luc infection or cell viability in A549 cells treated with candidate drugs (10 μmol/L). D, The relative cell viability in A549 cells treated with AZ (0.03125-320 μmol/L) for 72 h. E, The relative inhibitory rate of AZ (10 μmol/L), amantadine (10 μmol/L), oseltamivir (10 μmol/L) and ribavirin (10 μmol/L) on IAV-luc infection in A549 cells. F, The relative inhibitory rate of AZ (10 μmol/L), erythromycin (10 μmol/L), roxithromycin (10 μmol/L), midecamycin (10 μmol/L), spiramycin (10 μmol/L), acetylspiramycin (10 μmol/L), clarithromycin (10 μmol/L) and dirithromycin (10 μmol/L) on IAV-luc infection in A549 cells. G, The relative inhibitory rate of ethanol or AZ (2.5 or 5 μmol/L) on IAV-luc infection in HEK 293T/Hela/A549 cells. H, The relative mRNA level of *NP* in A549 cells treated with ethanol or AZ (2, 10, 50 μmol/L) and infected with WSN (MOI = 0.001 or 0.01) for 12 h. Solvent was treated as Ctrl. I, The dose-dependent relative inhibitory rate of AZ on WSN/H5N1/H7N9 pseudovirus infection in A549 cells. Solvent (Ethanol, DMSO or H_2O) was treated as control (Ctrl). All results are representative of three replicate experiments. ns, no significant, *$P < .05$, **$P < .01$, ***$P < .001$, ****$P < .0001$

contained: 125 mmol/L KCl, 25 mmol/L NaCl, 10 μmol/L monensin (Sigma), and 25 mmol/L HEPES (pH 7.5 or 7.0) or 25 mmol/L MES(pH 6.5, 6.0, 5.5, 5.0, 4.5, 4.0 or 3.5). To quantitatively analyse the effect of AZ on the acidification of endosome, we did dual-emission ratiometric measurement of pH using LysoSensor Yellow/Blue DND-160 (Shanghai YEASEN) as previously reported.[32] Briefly, A549 cells were seeded in 96-well plate at 5×10^4 cells per well. 12 hours later, A549 cells were pre-treated with the indicated drugs at 37°C for 2 hours, treated with 1 μmol/L DND-160 for 5 minutes and washed with PBS. Then, readouts of cell fluorescence relatively were recorded with a microplate reader (λ_{ex} = 329/384 nm, λ_{em} = 440/540 nm).

To further quantitatively analyse the effect of AZ on the acidification of vesicles containing virions, we fused pHluorin2 (enhanced, ratiometric, pH-sensitive green florescent protein) with N and C terminate of NPC1, which is specifically expressed in endosome and lysosome, and induced this fusion protein in A549 cell line with an tetracycline-inducible lentivirus system (Teton-3G) (Figure 5C,D). The A549 cells were seeded in confocal dish with glass bottom at 4×10^5 cells per well, and the expression of NPC1-pHluorin2 was induced with 10 μg/mL doxycycline for 24 hours. Then, the cells were pre-treated with the indicated drugs at 37°C for 2 hours and incubated with DiI-labelled WSN in infection medium at 4°C for 1 hour, and incubated at 37°C for 1 hour. After washing 3 times with PBS, the images were captured with confocal microscope (λ_{ex} = 405/488 nm, λ_{em} = 500-550 nm, Leica TCS SP8) and analysed with ImageJ (Image J_1.51j8).

2.12 | Statistical analysis

The results were presented as the mean ± SEM. The unpaired two-tail Student's t test was used to determine the statistical significance. A P-value < .05 was considered to be statistically significant. The Prism software program for Windows (GraphPad Software) was used to perform all calculations.

3 | RESULTS

3.1 | AZ is identified as a potential inhibitor of IAV in vitro

To rapidly and robustly screen candidate drugs with anti-IAV activity, a previously reported engineered replication-competent PR8 strain carrying luciferase reporter gene (IAV-luc) was used.[33] A549 cells were pre-treated with candidate drugs for 8 hours, and then, they were infected with IAV-luc. The supernatant was used in the luciferase assay 24 hours post-infection. The results demonstrated that, among these candidate drugs, AZ showed the most powerful inhibition on IAV-luc infection without significant cytotoxicity (Figure 1A-D). Compared with the FDA-approved anti-IAV drugs (amantadine, oseltamivir and ribavirin), AZ showed the same or even higher inhibitory activity to the IAV-luc reporter virus (Figure 1E). To determine whether other

macrolide type of antibiotics also possess anti-IAV activity, we detected the anti-IAV activity of multiple macrolide antibiotics, including AZ, erythromycin, roxithromycin, midecamycin, spiramycin, acetylspiramycin, clarithromycin and dirithromycin. While all these macrolide antibiotics significantly inhibited the IAV-luc infection, AZ is one of the most potent macrolide antibiotics with anti-IAV activity (Figure 1F). Consistently, AZ also inhibited the infection of IAV-luc in a number of cell lines of different histological origins (including 293T, Hela and A549 cell lines) and the infection of the wild-type WSN in A549 cell line (Figure 1G,H). To evaluate the antiviral activity of AZ to various IAV subtypes, we constructed WSN, H5N1 and H7N9 pseudovirus and found that AZ inhibited the infection rates of the pseudovirus of all three IAV subtypes (Figure 1I). Taken together, these results demonstrate that AZ could inhibit the infection of different IAV subtypes in different cell types.

3.2 | AZ has antiviral activity against SARS-CoV-2 pseudovirus in vitro

To screen the candidate anti-SARS-CoV-2 drugs in BSL-2 laboratory, we prepared the HIV- and MLV-based pesudovirus according to a previously reported method[34] with several modifications. As ACE2 has been identified as the host receptor of SARS-CoV and SARS-CoV-2,[35,36] we constructed the human ACE2 stable expressed HEK293T (HEK293T-ACE2) with lentiviral mediated gene transduction. Consistent with reported studies, package of MLV-based pseudovirus is more efficient than HIV-based pseudovirus in both SARS-CoV and SARS-CoV-2 (Figure 2A). So the MLV-based pseudovirus model was chosen in subsequent experiments. Given the antiviral activity of macrolide antibiotics in IAV and other virus species, we tested them in the SARS-CoV-2 MLV-based pesudovirus model. Similar with IAV model, CQ, NH_4Cl and all eight macrolide antibiotics (AZ, erythromycin, roxithromycin, midecamycin, spiramycin, acetylspiramycin, clarithromycin and dirithromycin) showed significant anti-SARS-CoV-2 activities in HEK293T-ACE2 cells (Figure 2B). With VSV and Ebola HIV-based pseudovirus models and SARS-CoV and SARS-CoV-2 MLV-based pseudovirus models, we found that AZ could effectively inhibit the infection of SARS-CoV, SARS-CoV-2 and Ebola pseudovirus activity without significant cytotoxicity, but show much less efficiency in VSV pseudovirus (Figure 2C-G). With the GFP marked SeV, VSV and HSV-1, we also observed antiviral activities of AZ against SeV and VSV, but not HSV-1 (Figure S1). The EC_{50} of AZ in SARS-CoV, SARS-CoV-2 and Ebola pseudovirus model was lower than 0.625 μmol/L. Moreover, the antiviral activity of AZ was verified in Caco2 cell line which is naturally susceptible to SARS-CoV-2 (Figure 2H). In order to explore the potential of AZ to inhibit various SARS-CoV-2 mutant strains, we constructed sixteen currently circulating spike protein mutations (L5F, D215H, S247R, F342L, N354D, D364Y, N354D + D364Y, V367F, R408I, W436R, G476S, V483A, D614G, V622I, Q675H and R682Q). Similar with WT pseudovirus, AZ could also significantly inhibit the infection of all sixteen pseudovirus with mutant spike protein in HEK293-ACE2 cells (Figure 2I).
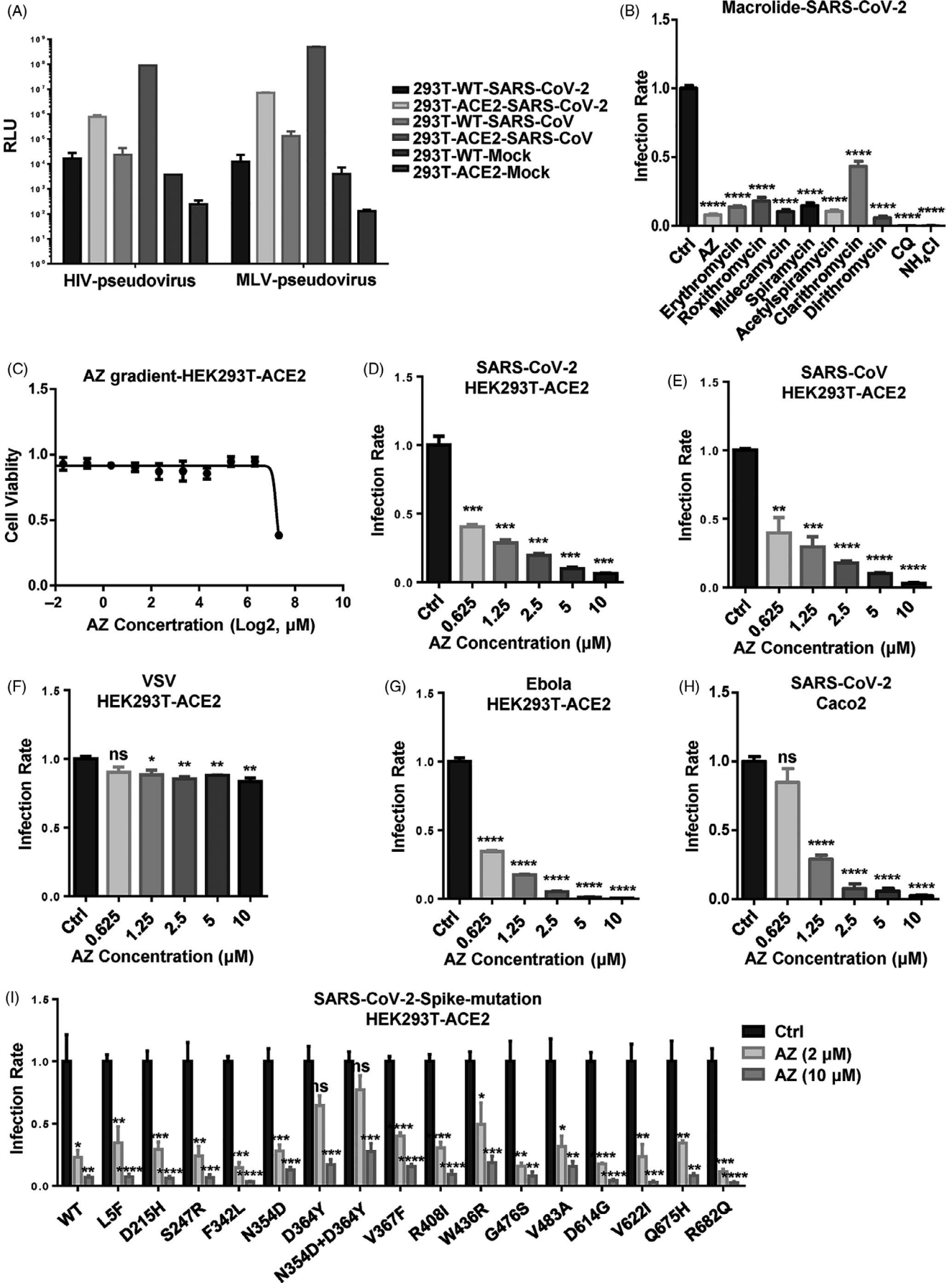
FIGURE 2 AZ has antiviral activity against SARS-CoV-2 pseudovirus in vitro. A, The infectivities of SARS-CoV and SARS-CoV-2 pseudovirus in WT and human ACE2 stably expressed HEK293T cells. B, The relative inhibitory rate of AZ (10 µmol/L), erythromycin (10 µmol/L), roxithromycin (10 µmol/L), midecamycin (10 µmol/L), spiramycin (10 µmol/L), acetylspiramycin (10 µmol/L), clarithromycin (10 µmol/L), dirithromycin (10 µmol/L), chloroquine (CQ, 10 µmol/L) and NH$_4$Cl (10 mmol/L) on SARS-CoV-2 pseudovirus infection in HEK293T-ACE2 cells. C, The relative cell viability of HEK293T-ACE2 cells treated with AZ (0.15625-160 µmol/L) for 72 h. D-G, The relative inhibitory rate on SARS-CoV-2, SARS-CoV, VSV and Ebola pseudovirus infection in HEK293T-ACE2 cells treated with AZ (0.625-10 µmol/L). H, The relative inhibitory rate on SARS-CoV-2 pseudovirus infection in Caco2 cells treated with AZ (0.625-10 µmol/L). I, The relative inhibitory rate on WT and mutant SARS-CoV-2 pseudovirus infection in HEK293T-ACE2 cells treated with AZ (2 and 10 µmol/L). Solvent was treated as Ctrl. Experiments were repeated twice. ns, no significant, *P < .05, **P < .01, ***P < .001, ****P < .0001

FIGURE 3 AZ can exert its antiviral effect independently of the activation of interferon pathway. A, The relative infection rate of IAV-luc in WT or IFNAR1 KO HEK293T cells 24 h post-infection. B, The relative inhibitory rate of IAV-luc infection in WT or IFNAR1 KO HEK293T cells treated by IFN-beta (10 ng/mL) or AZ (10 µmol/L) 24 h post-infection. C, The relative inhibitory rate of IAV-luc infection in WT or RIG-I KO HEK293T cells treated by AZ (2.5 µmol/L) 24 h post-infection. D-F, The relative mRNA level of *IFNB1*, *ISG54* and *CCL5* in A549 cells treated with ethanol or AZ (2, 10, 50 µmol/L) and stimulated with WSN for 12 h. Solvent was treated as Ctrl. All results are representative of three replicate experiments. ns, no significant, *P < .05, **P < .01, ***P < .001, ****P < .0001
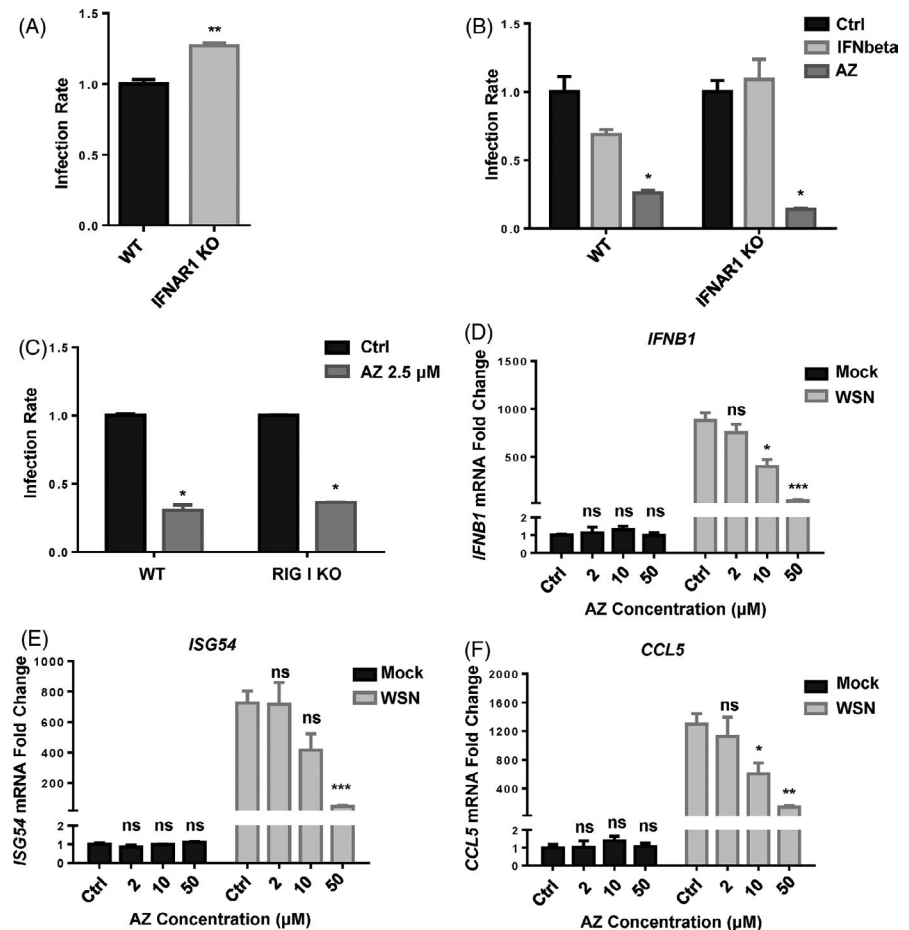
Our results thus identified AZ as a potential anti-SARS-CoV-2 candidate drug in vitro.

3.3 | AZ exerts its antiviral effect independently of the activation of interferon pathway

As the key components of innate antiviral immunity, interferons exert antiviral effects by inducing hundreds of ISG, which possess various antiviral functions through different modes of action.[37] To verify whether AZ exerts antiviral effect by activating interferon signalling, we detected the antiviral effect of AZ in HEK293T cells with an interferon-defected pathway (IFNAR1 KO and RIG-I KO). Consistent with a previous study, knockout of IFNAR1 facilitated IAV-luc infection and replication significantly (Figure 3A). While interferon-β did not inhibit IAV-luc infection in IFNAR KO HEK293T cells as effectively as

in WT HEK293T cells, AZ showed the same degree of antiviral effect to IAV-luc infection in both cells (Figure 3B). Similarly, AZ also inhibited the IAV-luc infection in RIG-I KO HEK293T cells as effectively as in WT HEK293T cells (Figure 3C). Moreover, AZ alone did not affect the *IFNβ* or ISG (*ISG54*, *CCL5*) mRNA levels in A549 cells, but it dose-dependently inhibited the increase of mRNA levels of *IFNβ*, *ISG54* and *CCL5* stimulated by WSN infection in A549 (Figure 3D-F). Taken together, these results prove that the major part, if not all, of the antiviral effect of AZ is independent of the interferon signalling.

3.4 | AZ inhibits IAV infection by interfering with the acidification of vesicles

AZ treatment inhibited the infection of replication-competent and pseudotyped IAV, demonstrating that AZ probably targets the entry

phase of IAV (Figure 1H). To exclude the effect of AZ on IAV replication, we used IAV minigenome system (vRNP complex) to evaluate the effect of AZ on RNA polymerase activity. In contrast with favipiravir and ribavirin (viral RNA synthesis inhibitors), AZ did not affect the RNA polymerase activity of IAV (Figure 4A). The time course experiment demonstrated that addition of AZ at hour post-infection (h.p.i.) 2, but not h.p.i. 4, still inhibited the infection of WSN pseudovirus, implying that AZ may act at the late phase of IAV entry (Figure 4B). To locate the precise phase of infection at which AZ blocks the IAV infection process, we examined the effects of AZ on IAV binding, internalization, acidification and membrane fusion. As the first phase of IAV infection, binding of IAV to A549 cell membrane was not affected by AZ treatment (Figure 4C). Moreover, the co-localization of Dil-labelled IAV with RAB5A- or RAB7A-positive endosomes was not affected, implying AZ did not block the internalization of IAV to early endosome or late endosome at where the nucleocapsid of IAV is released into the cytoplasm (Figure 4D). As the key to induce hemagglutinin (HA) conformational changes and initiate fusion of viral and vacuolar membranes, acidification of vesicles was detected by lyso-tracker red staining. Similar with the well-known acidification inhibitors (chloroquine, bafilomycin A1 and ammonium chloride), AZ significantly decreased the lyso-tracker red staining, indicating that the acidification of vesicles was inhibited by AZ treatment (Figure 4E,F). Consistently, a lipophilic dye-based fluorescence dequenching assay using R18 (red) and SP-DiOC18 (green, fixable) demonstrated that the fusion of viral and vacuolar membranes was also inhibited by AZ treatment (Figure 4G,H). Moreover, these membrane fusion results are consistent with the pseudovirus assay (Figure 4I). Therefore, our data demonstrate that the antiviral effect of AZ relies on the alkalinization of acid vesicles to inhibit the IAV entry.

3.5 | AZ inhibits the acidification of vesicles containing IAV virions

Measured HA activation pH values across all subtypes and species range from 4.6 to 6.0.[38] To quantify the alkalinization of acidic vesicles by AZ treatment, LysoSensor Yellow/Blue DND-160, a ratiometric pH sensing dye, was used to quantify the pH of acidic vesicles.

Similar to bafilomycin A1 and NH_4Cl, AZ could dose-dependently increase the pH value of acidic vesicles (Figure 5A-B). However, this result only showed the average pH of all the acidic vesicles (including early endosome, recycled endosome, late endosome, lysosome, autophagosome, golgi), but not the specific vesicles where IAV locate. To specifically evaluate the effect of AZ on the pH of vesicles containing IAV, we constructed an A549 cell line with endosomal and lysosomal expression of pHluorin2 (an enhanced, ratiometric, pH-sensitive GFP variant).[39] We fused pHluorin2 with the N terminal (signal peptide), transmembrane region 1 (TM1) and C terminal (C-tail) of NPC1, which is expressed specifically in the endosome and lysosome (Figure 5C-E). Consistent with LysoSensor Yellow/Blue DND-160 assay, pHluorin2 assay indicated that AZ treatment significantly increased the pH of NPC1-labelled endosome and lysosome (Figure 5F). Further, we specifically detected the pH of vesicles containing Dil-labelled IAV and found that AZ treatment significantly alkalized the vesicles containing Dil-labelled IAV (Figure 5G). Thus, AZ treatment could alkalize the vesicles containing IAV virions out of the proper pH rang of HA activation.

4 | DISCUSSION

In this study, we identified that AZ exhibited a powerful antiviral effect against various IAV subtypes, including H1N1, H5N1 and H7N9. Excitingly, AZ also possesses in vitro anti-SARS-CoV-2 and anti-SARS-CoV activities in pseudovirus inhibition assays. As AZ has also reported having antiviral effects against rhinovirus, Ebola virus and Zika virus,[22-25,40] AZ is therefore a highly promising candidate of broad-spectrum antiviral agents. With the pseudotyped IAV and minigenome models, we found that AZ inhibited the entry, but not the replication of the IAV. Moreover, the binding of IAV to cell membrane and the internalization of IAV into late endosome were not affected, but AZ treatment inhibited the acidification of the vesicles containing IAV and the fusion of viral and endosomal membranes.

In view of the antibiotic and immunomodulatory activities of AZ, it may have a favourable effect on the infectious diseases, such as influenza and COVID-19. Based on this tentative idea, some clinical trials have been carried out examine the therapeutic potential of AZ against influenza virus and SARS-CoV-2 infection. Compared

FIGURE 4 AZ inhibits IAV infection by interfering with the acidification of vesicles. A, The relative luciferase activity of IAV minigenome system treated by favipiravir (10 μmol/L), ribavirin (10 μmol/L) or AZ (10 μmol/L) 24 h post-treatment (n = 3 per group). Minigenome system without NP vector was indicated as negative control (NC). B, The time course of relative inhibitory rate of AZ on WSN pseudovirus infection in A549 cells from h.p.i. −8 to 8 (n = 8 per group). C, The representative image of A549 infected by Dil-labelled WSN (up panel), the quantitative analysis of the number of Dil-labelled WSN per cell (down panel). Scale bar, 10 μm. D, Co-localization of EGFP-RAB5A/RAB7A and Dil-labelled WSN in A549 treated with ethanol or AZ (10 μmol/L) 1 h post-WSN infection, white arrows indicate the examples of co-localization. Scale bar, 10 μm. E and F, The representative image and quantitative analysis of lyso-tracker red staining in A549 treated with AZ (10 μmol/L), chloroquine (CQ, 10 μmol/L), bafilomycin A1 (Baf A1, 50 nmol/L) or ammonium chloride (NH_4Cl, 10 mmol/L) for 2 h (n ≥ 3 per group). Scale bar, 10 μm. G and H, The representative image and quantitative analysis of viral and vacuolar membranes fusion in A549 treated with ethanol, AZ (10 μmol/L), chloroquine (CQ, 10 μmol/L), bafilomycin A1 (Baf A1, 50 nmol/L) or ammonium chloride (NH_4Cl, 10 mmol/L) for 2 h, and infected with R18/SP-Dioc18 labelled WSN for 1h (n ≥ 3 per group). Scale bar, 10 μm. I, The relative inhibitory rate of AZ (10 μmol/L), chloroquine (CQ, 10 μmol/L), bafilomycin A1 (Baf A1, 50 nmol/L) or ammonium chloride (NH_4Cl, 10mM) on WSN pseudovirus infection in A549 cells. Solvent was treated as Ctrl. ns, no significant, *$P < .05$, **$P < .01$, ***$P < .001$, ****$P < .0001$
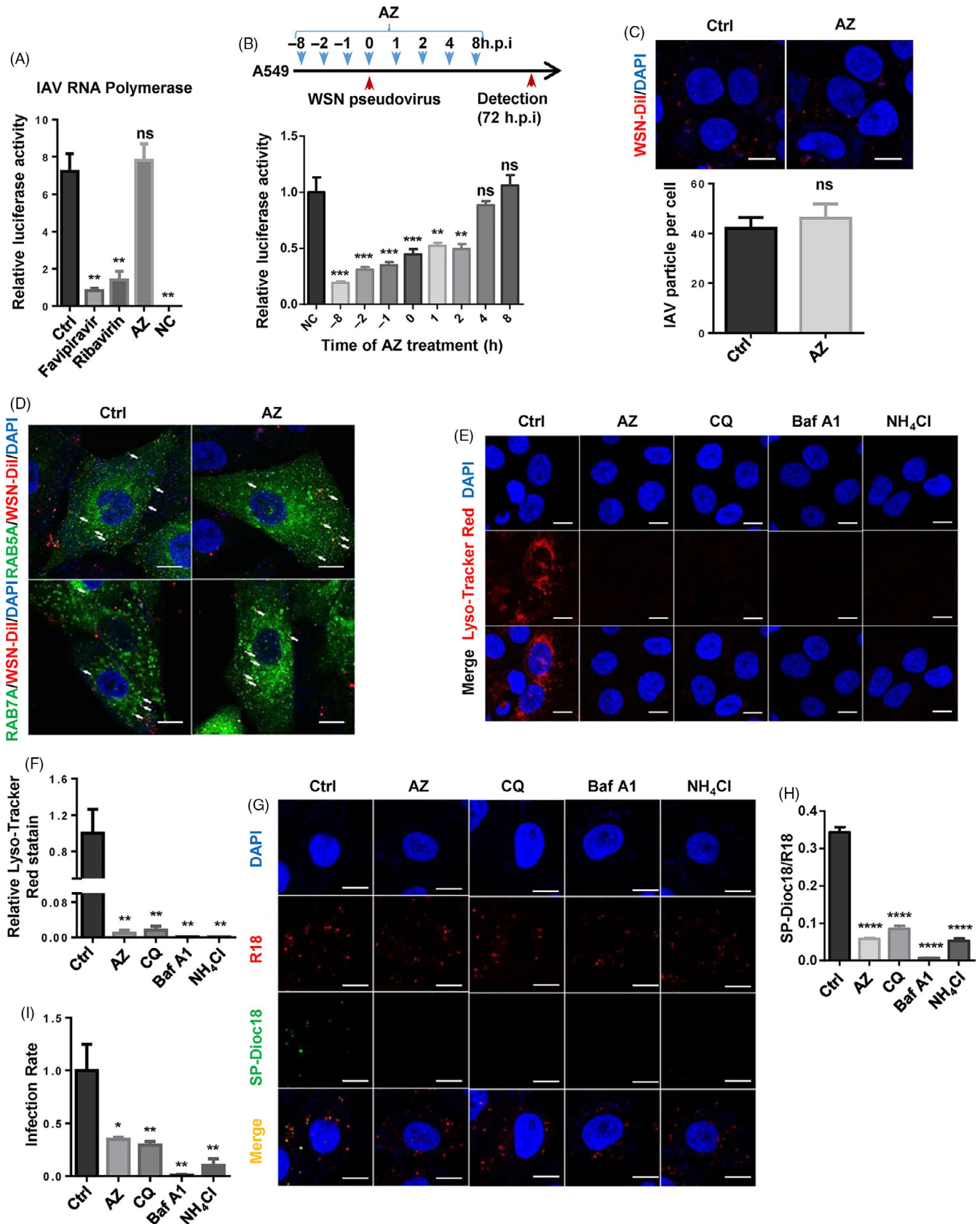
with oseltamivir monotherapy, combination therapy (oseltamivir plus AZ) did not significantly affect the inflammatory cytokine expression level, but showed an early resolution of some symptoms in influenza patients, implying this favourable effect of AZ maybe independent of its immunomodulatory activity.[41] Since the outbreak of this epidemic, some studies have reported the favourable effect
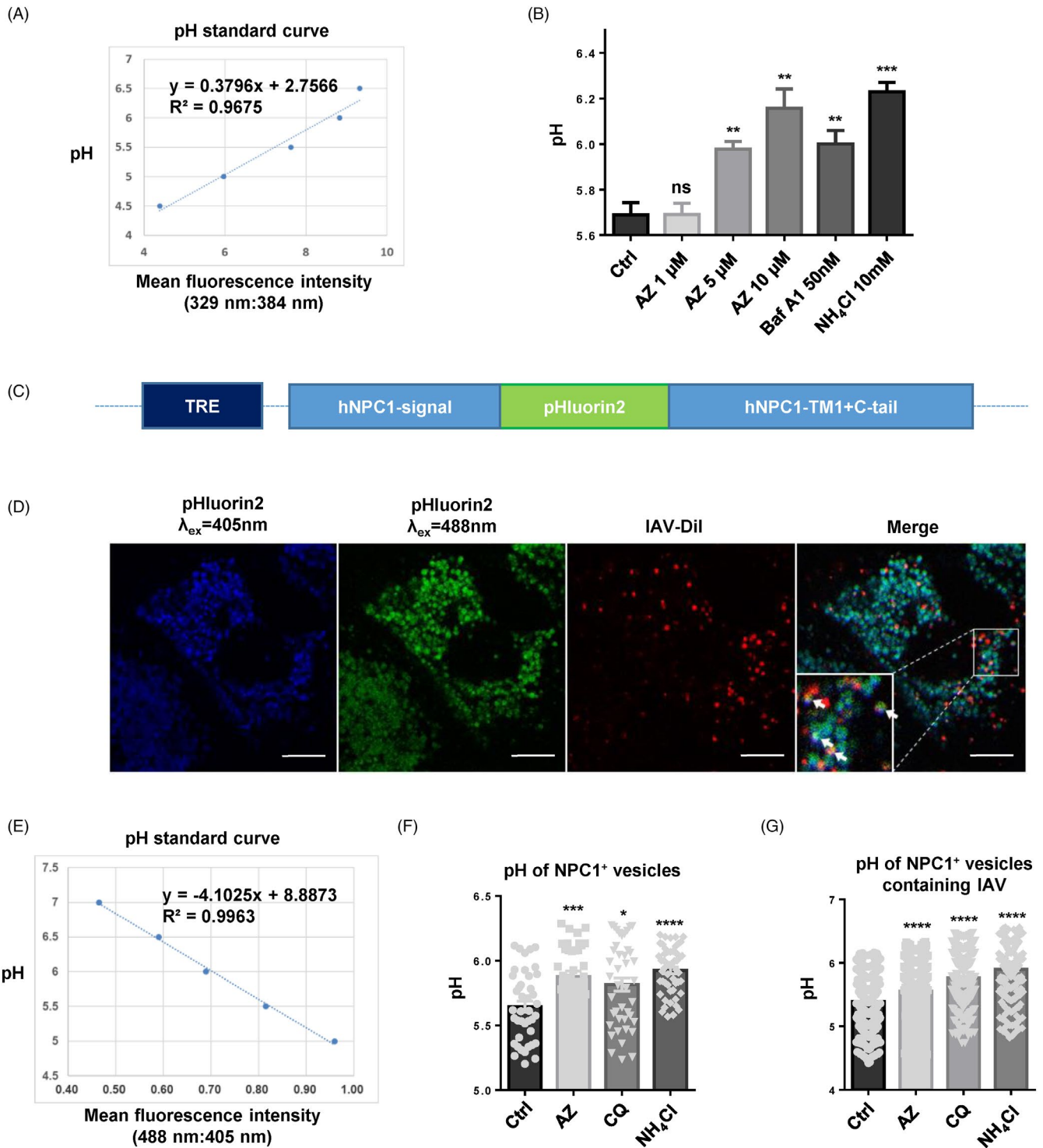
FIGURE 5 AZ inhibits the acidification of vesicles containing IAV virions. A, The pH standard curve of LysoSensor Yellow/Blue DND-160 assay in A549 cells. B, The increase of pH by AZ (1, 5, 10 μmol/L), Baf A1 (50 nmol/L) and NH₄Cl (10 mmol/L) in A549 cells with the LysoSensor Yellow/Blue DND-160 assay. C, Schematic diagram of NPC1-pHluorin2 expression vector. D, The representative image of NPC1-pHluorin2 A549 cells infected with DiI-labelled WSN virus for 1 h. Scale bar, 10 μm. E, The pH standard curve of NPC1-pHluorin2 assay in A549 cells. F, The pH increase of NPC1 + vesicles by AZ (10 μmol/L), CQ (10 μmol/L) and NH₄Cl (10 mmol/L) in NPC1-pHluorin2 A549 cells induced with doxycycline. G, The pH increase of NPC1 + vesicles containing DiI-labelled WSN virus by AZ (10 μmol/L), CQ (10 μmol/L) and NH₄Cl (10 mmol/L) in NPC1-pHluorin2 A549 cells induced with doxycycline. Solvent was treated as Ctrl. All results are representative of three replicate experiments. ns, no significant, $*P < .05$, $**P < .01$, $***P < .001$, $****P < .0001$

of AZ combined with hydroxychloroquine (HCQ) against SARS-CoV-2 in vitro and in vivo.[8,42-44] However, other studies reported inconsistent results and adverse effects of HCQ and AZ in COVID-19 patients.[45-47] Therefore, more comprehensive clinical and basic research is needed to clarify the anti-SARS-CoV-2 effect of AZ.

As reported in rhinovirus and Zika virus study, AZ treatment also increased the virus-induced interferon mRNA expression,[26,48-50] implying that AZ may exert anti-IAV activity partially through activation of the interferon signalling induced by IAV infection. However, the defection of interferon signalling did not affect the antiviral effect of AZ (Figure 3B,C), suggesting that the interferon-mediated anti-IAV effect of AZ is dispensable. Moreover, AZ alone did not affect the mRNA level of IFNβ or ISGs, but inhibited the increase of mRNA level stimulated by WSN infection, which is presumably due to the less nucleocapsid released into the cytoplasm (Figure 3D-F). Inconsistencies of interferon mRNA expression between these studies are presumably due to the difference of virus classification and the host cells.

As reported in the recently published literature,[51] SARS-CoV-2 pseudovirus entries into the HEK293T-ACE2 mainly through endocytosis, which is regulated by PIKfyve, TPC2 and cathepsin L. Moreover, it has been shown that SARS-CoV S-pseudotyped virions use the endosomal protease cathepsin L to infect cells.[52,53] Therefore, the activity of cathepsin L (a lysosomal acid cysteine protease) could be weakened by the alkalinization of endo-lysosome, which is consistent with our results that chloroquine and ammonium chloride almost completely suppress SARS-CoV-2 pseudovirus infection in HEK293T-ACE2 (Figure 2B). Therefore, proper acidic environment maybe a limiting factor for SARS-CoV-2, but this should be verified with live virus and in more cell models.

Recently, it is reported that AZ inhibits influenza A (H1N1) pdm09 virus infection by interfering with virus internalization process,[54] but the concentration of AZ (200 μmol/L) is too high to exclude the possibility of non-specific effect on transport of endosome. In our study, we proved that a relatively low dose of AZ (10 μmol/L) does not inhibit the internalization of IAV, but the acidification of endosomes, which is a key limiting factor for various influenza virus and some enveloped virus infection (maybe including SARS-CoV-2). While bafilomycin A1, a macrolide antibiotic, is identified as a specific inhibitor of vacuolar-type H^+-ATPase and could suppress the replication of IAV in human lung epithelial cells,[55-57] the mechanism by which AZ alkalizes the acidic vesicles is still undefined. In view of the physical and chemical properties of AZ (pKa = 8.74, logP = 4.02), it belongs to the cationic amphiphilic drugs (CAD), which could accumulate in and alkalize acid vesicles.[58] Therefore, AZ may act as a weak base to prevent the acidification of the endosome. However, this hypothesis needs to be carefully verified.

As a critical host factor hijacked by several enveloped viruses, proper acidic environment is a limiting factor for conformation change and/or priming of fusion mediating glycoprotein, suggesting the acidification of endosome and lysosome could be a potential target for antiviral drug development. Unlike to targeting viral proteins, targeting the host factors speculatively possesses a lower likelihood of drug resistance.[59] Therefore, by targeting the acidification of endosome and lysosome, AZ could possess a broad-spectrum antiviral effect and higher barrier to drug resistance.

In summary, we identified AZ as a broad-spectrum antiviral against IAV and SARS-CoV-2, and a potential clinical anti-SARS-CoV-2 drug used for emergency and a promising candidate for the development of clinical anti-IAV drug.

CONFLICTS OF INTERESTS

The authors declare no competing financial interests.

AUTHOR CONTRIBUTION

XD, XZ, FM, CH, WO, YH, YG and XZ performed the experiments; XD, XZ, FX and FXQ analysed data and wrote the manuscript; and FX and FXQ was responsible for research design, strategy and supervision.

DATA AVAILABILITY STATEMENT

The data that support the findings of this study are available from the corresponding author upon reasonable request.

ORCID

Feng Xu https://orcid.org/0000-0001-5764-6628
Frank Xiaofeng Qin https://orcid.org/0000-0002-5395-0304

REFERENCES

1. Pleschka S. Overview of influenza viruses. *Curr Top Microbiol Immunol*. 2013;370:1-20.
2. Asha K, Kumar B. Emerging influenza D virus threat: what we know so far! *J Clin Med*. 2019;8:192.
3. Park JE, Ryu Y. Transmissibility and severity of influenza virus by subtype. *Infect Genet Evol*. 2018;65:288-292.
4. Drosten C, Gunther S, Preiser W, et al. Identification of a novel coronavirus in patients with severe acute respiratory syndrome. *N Engl J Med*. 2003;348:1967-1976.
5. Zaki AM, van Boheemen S, Bestebroer TM, Osterhaus AD, Fouchier RA. Isolation of a novel coronavirus from a man with pneumonia in Saudi Arabia. *N Engl J Med*. 2012;367:1814-1820.
6. Zhu N, Zhang D, Wang W, et al. A novel coronavirus from patients with pneumonia in China, 2019. *N Engl J Med*. 2020;382:727-733.
7. Wang M, Cao R, Zhang L, et al. Remdesivir and chloroquine effectively inhibit the recently emerged novel coronavirus (2019-nCoV) in vitro. *Cell Res*. 2020;30:269-271.
8. Gautret P, Lagier JC, Parola P, et al. Hydroxychloroquine and azithromycin as a treatment of COVID-19: results of an open-label non-randomized clinical trial. *Int J Antimicrob Agents*. 2020;56:105949.
9. Gautret P, Lagier JC, Parola P, et al. Clinical and microbiological effect of a combination of hydroxychloroquine and azithromycin in 80 COVID-19 patients with at least a six-day follow up: a pilot observational study. *Trav Med Infect Dis*. 2020;34:101663.
10. Loregian A, Mercorelli B, Nannetti G, Compagnin C, Palu G. Antiviral strategies against influenza virus: towards new therapeutic approaches. *Cell Mol Life Sci*. 2014;71:3659-3683.
11. Han J, Perez J, Schafer A, et al. Influenza virus: small molecule therapeutics and mechanisms of antiviral resistance. *Curr Med Chem*. 2018;25:5115-5127.
12. Yen HL. Current and novel antiviral strategies for influenza infection. *Curr Opin Virol*. 2016;18:126-134.

13. Kim H, Webster RG, Webby RJ. Influenza virus: dealing with a drifting and shifting pathogen. *Viral Immunol*. 2018;31:174-183.

14. Lambert LC, Fauci AS. Influenza vaccines for the future. *N Engl J Med*. 2010;363:2036-2044.

15. Wong SS, Webby RJ. Traditional and new influenza vaccines. *Clin Microbiol Rev*. 2013;26:476-492.

16. Pushpakom S, Iorio F, Eyers PA, et al. Drug repurposing: progress, challenges and recommendations. *Nat Rev Drug Discovery*. 2019;18:41-58.

17. Chinali G, Nyssen E, Di Giambattista M, Cocito C. Inhibition of polypeptide synthesis in cell-free systems by virginiamycin S and erythromycin. Evidence for a common mode of action of type B synergimycins and 14-membered macrolides. *Biochem Biophys Acta*. 1988;949:71-78.

18. Khair OA, Devalia JL, Abdelaziz MM, Sapsford RJ, Davies RJ. Effect of erythromycin on Haemophilus influenzae endotoxin-induced release of IL-6, IL-8 and sICAM-1 by cultured human bronchial epithelial cells. *Eur Respir J*. 1995;8:1451-1457.

19. Takizawa H, Desaki M, Ohtoshi T, et al. Erythromycin suppresses interleukin 6 expression by human bronchial epithelial cells: a potential mechanism of its anti-inflammatory action. *Biochem Biophys Res Comm*. 1995;210:781-786.

20. Takizawa H, Desaki M, Ohtoshi T, et al. Erythromycin modulates IL-8 expression in normal and inflamed human bronchial epithelial cells. *Am J Respir Crit Care Med*. 1997;156:266-271.

21. Tamaoki J, Sakai N, Tagaya E, Konno K. Macrolide antibiotics protect against endotoxin-induced vascular leakage and neutrophil accumulation in rat trachea. *Antimicrob Agents Chemother*. 1994;38:1641-1643.

22. Jang YJ, Kwon HJ, Lee BJ. Effect of clarithromycin on rhinovirus-16 infection in A549 cells. *Eur Respir J*. 2006;27:12-19.

23. Suzuki T, Yamaya M, Sekizawa K, et al. Bafilomycin A(1) inhibits rhinovirus infection in human airway epithelium: effects on endosome and ICAM-1. *Am J Physiol Lung Cell Mol Physiol*. 2001;280:L1115-1127.

24. Suzuki T, Yamaya M, Sekizawa K, et al. Erythromycin inhibits rhinovirus infection in cultured human tracheal epithelial cells. *Am J Respir Crit Care Med*. 2002;165:1113-1118.

25. Retallack H, Di Lullo E, Arias C, et al. Zika virus cell tropism in the developing human brain and inhibition by azithromycin. *Proc Natl Acad Sci USA*. 2016;113:14408-14413.

26. Li C, Zu S, Deng YQ, et al. Azithromycin protects against Zika virus infection by upregulating virus-induced type I and III interferon responses. *Antimicrob Agents Chemother*. 2019;63:e00394-19.

27. Fan H, Du X, Zhang J, et al. Selective inhibition of Ebola entry with selective estrogen receptor modulators by disrupting the endolysosomal calcium. *Sci Rep*. 2017;7:41226.

28. Bortz E, Westera L, Maamary J, et al. Host- and strain-specific regulation of influenza virus polymerase activity by interacting cellular proteins. *MBio*. 2011;2:e00151-11.

29. Sakai T, Ohuchi M, Imai M, et al. Dual wavelength imaging allows analysis of membrane fusion of influenza virus inside cells. *J Virol*. 2006;80:2013-2018.

30. Xinhan L, Matsushita M, Numaza M, Taguchi A, Mitsui K, Kanazawa H. Na+/H+ exchanger isoform 6 (NHE6/SLC9A6) is involved in clathrin-dependent endocytosis of transferrin. *Am J Physiol Cell Physiol*. 2011;301:C1431-C1444.

31. Ouyang Q, Lizarraga SB, Schmidt M, et al. Christianson syndrome protein NHE6 modulates TrkB endosomal signaling required for neuronal circuit development. *Neuron*. 2013;80:97-112.

32. Ma L, Ouyang Q, Werthmann GC, Thompson HM, Morrow EM. Live-cell microscopy and fluorescence-based measurement of luminal pH in intracellular organelles. *Front Cell Dev Biol*. 2017;5:71.

33. Pan W, Dong Z, Li F, et al. Visualizing influenza virus infection in living mice. *Nat Commun*. 2013;4:2369.

34. Giroglou T, Cinatl J Jr, Rabenau H, et al. Retroviral vectors pseudotyped with severe acute respiratory syndrome coronavirus S protein. *J Virol*. 2004;78:9007-9015.

35. Hoffmann M, Kleine-Weber H, Schroeder S, et al. SARS-CoV-2 Cell entry depends on ACE2 and TMPRSS2 and is blocked by a clinically proven protease inhibitor. *Cell*. 2020;181:271-280.e8.

36. Lan J, Ge J, Yu J, et al. Structure of the SARS-CoV-2 spike receptor-binding domain bound to the ACE2 receptor. *Nature*. 2020;581:215-220.

37. Schneider WM, Chevillotte MD, Rice CM. Interferon-stimulated genes: a complex web of host defenses. *Annu Rev Immunol*. 2014;32:513-545.

38. Scholtissek C. Stability of infectious influenza A viruses at low pH and at elevated temperature. *Vaccine*. 1985;3:215-218.

39. Mahon MJ. pHluorin2: an enhanced, ratiometric, pH-sensitive green florescent protein. *Adv Biosci Biotechnol*. 2011;2:132-137.

40. Madrid PB, Panchal RG, Warren TK, et al. Evaluation of Ebola virus inhibitors for drug repurposing. *ACS Infect Dis*. 2015;1:317-326.

41. Kakeya H, Seki M, Izumikawa K, et al. Efficacy of combination therapy with oseltamivir phosphate and azithromycin for influenza: a multicenter, open-label, randomized study. *PLoS One*. 2014;9:e91293.

42. Andreani J, Le Bideau M, Duflot I, et al. In vitro testing of combined hydroxychloroquine and azithromycin on SARS-CoV-2 shows synergistic effect. *Microb Pathog*. 2020;145:104228.

43. Sekhavati E, Jafari F, SeyedAlinaghi S, et al. Safety and effectiveness of azithromycin in patients with COVID-19: an open-label randomised trial. *Int J Antimicrob Agents*. 2020;56:106143.

44. Million M, Lagier JC, Gautret P, et al. Early treatment of COVID-19 patients with hydroxychloroquine and azithromycin: a retrospective analysis of 1061 cases in Marseille, France. *Trav Med Infect Dis*. 2020;35:101738.

45. Molina JM, Delaugerre C, Le Goff J, et al. No evidence of rapid antiviral clearance or clinical benefit with the combination of hydroxychloroquine and azithromycin in patients with severe COVID-19 infection. *Med Mal Infect*. 2020;50:384.

46. Rosenberg ES, Dufort EM, Udo T, et al. Association of treatment with hydroxychloroquine or azithromycin with in-hospital mortality in patients with COVID-19 in New York State. *JAMA*. 2020;323:2493-2502.

47. Saleh M, Gabriels J, Chang D, et al. Effect of chloroquine, hydroxychloroquine, and azithromycin on the corrected QT interval in patients with SARS-CoV-2 infection. *Circ Arrhyth Electrophysiol*. 2020;13:e008662.

48. Gielen V, Johnston SL, Edwards MR. Azithromycin induces anti-viral responses in bronchial epithelial cells. *Eur Respir J*. 2010;36:646-654.

49. Menzel M, Akbarshahi H, Bjermer L, Uller L. Azithromycin induces anti-viral effects in cultured bronchial epithelial cells from COPD patients. *Sci Rep*. 2016;6:28698.

50. Schögler A, Kopf BS, Edwards MR, et al. Novel antiviral properties of azithromycin in cystic fibrosis airway epithelial cells. *Eur Respir J*. 2015;45:428-439.

51. Ou X, Liu Y, Lei X, et al. Characterization of spike glycoprotein of SARS-CoV-2 on virus entry and its immune cross-reactivity with SARS-CoV. *Nat Commun*. 2020;11:1620.

52. Simmons G, Gosalia DN, Rennekamp AJ, Reeves JD, Diamond SL, Bates P. Inhibitors of cathepsin L prevent severe acute respiratory syndrome coronavirus entry. *Proc Natl Acad Sci USA*. 2005;102:11876-11881.

53. Huang I-C, Bosch BJ, Li F, et al. SARS coronavirus, but not human coronavirus NL63, utilizes cathepsin L to infect ACE2-expressing cells. *J Biol Chem*. 2006;281:3198-3203.

54. Tran DH, Sugamata R, Hirose T, et al. Azithromycin, a 15-membered macrolide antibiotic, inhibits influenza A(H1N1)pdm09 virus

infection by interfering with virus internalization process. *J Antibiot.* 2019;72:759-768.

55. Swallow CJ, Grinstein S, Rotstein OD. A vacuolar type H(+)-ATPase regulates cytoplasmic pH in murine macrophages. *J Biol Chem.* 1990;265:7645-7654.

56. Crider BP, Xie XS, Stone DK. Bafilomycin inhibits proton flow through the H+ channel of vacuolar proton pumps. *J Biol Chem.* 1994;269:17379-17381.

57. Yeganeh B, Ghavami S, Kroeker AL, et al. Suppression of influenza A virus replication in human lung epithelial cells by noncytotoxic concentrations bafilomycin A1. *Am J Physiol Lung Cell Mol Physiol.* 2015;308:L270-L286.

58. Funk RS, Krise JP. Cationic amphiphilic drugs cause a marked expansion of apparent lysosomal volume: implications for an intracellular distribution-based drug interaction. *Mol Pharm.* 2012;9:1384-1395.

59. Edinger TO, Pohl MO, Stertz S. Entry of influenza A virus: host factors and antiviral targets. *J Gen Virol.* 2014;95:263-277.

SUPPORTING INFORMATION

Additional supporting information may be found online in the Supporting Information section.